Case History Studies of Lenihan and Austrian Dams under the 1989 Loma Prieta Earthquake

Guoxi Wu, Ph.D., P.Eng.[1]

[1]Specialist Engineer, Engineering Dept., BC Hydro; Wutec Geotechnical International.
Email: Guoxi.wu@bchydro.com; gwu@wutecgeo.com

ABSTRACT

Dynamic responses of the Lenihan and Austrian Dams in the 1989 Mw = 6.93 Loma Prieta earthquake were analyzed using the finite element program VERSAT; undrained response of the saturated dam fills was modelled using a total stress approach. The two dams were constructed in the early 1950s and comprised primarily of compacted low plasticity clayey sands and clayey gravels. Subjected to estimated peak accelerations of 0.44 g at Lenihan Dam and 0.55–0.6 g at Austrian Dam, the dams developed some to extensive longitudinal cracks on the dam faces and settled at the dam crest on average 0.25 m at Lenihan Dam and 0.76 m at Austrian Dam. This study demonstrates the robustness of the adopted approach in capturing the embankment dam's key performance under large earthquakes. The nonlinear response history analyses indicate that the proposed S_u/σ'_m approach for calculating in situ undrained shear strengths can be a reasonably conservative approach for engineering analysis and design. The calculated dam crest settlements for both dams are in good agreement with the dam crest settlements observed in the 1989 earthquake.

INTRODUCTION

The 61-m high Lenihan dam and the 55-m high Austrian dam, both constructed in the early 1950s, are compacted earthfill dams located in California. Both earthen embankment dams consisted primarily of low plasticity clayey sands and clayey gravels, whereas the lower core (Zone 2L) of Lenihan Dam was comprised of highly plastic sandy clays to silty sands or sandy silts. Subjected to earthquake ground motions of the 1989 Mw = 6.93 Loma Prieta earthquake with estimated horizontal peak ground accelerations (PGAs) of 0.55-0.6g at bedrock, the Austrian dam settled 0.76 m on average at its crest, developed extensive longitudinal cracks (up to 300 mm wide in one location) on both the upstream and downstream faces of the dam. The observed and measured dam displacements suggested that the dam had earthquake-induced internal movements related to lateral spreading of dam (Wahler Associates 1990; Harder et al. 1998). The Lenihan dam, about 10 km downstream of the Austrian dam and subjected to ground shaking of about 0.44g at the bedrock, developed longitudinal cracks on the dam faces and settled at its crest 0.25 m on average.

The total stress method of analysis, using the Mohr Coulomb failure criterion and various forms of hysteretic stress-strain relations, is a common method for dynamic analysis of undrained response involving clayey or cohesive soils; it is widely used in geotechnical engineering (Wu 2015; Sweeney and Yan 2014). The effective stress method of analysis, including calculation of earthquake-induced pore water pressure (PWP) during shaking and impact of the PWP on soil stiffness and strength, is becoming a standard approach for undrained response history analysis of sandy soils involving soil liquefaction and its induced large ground

deformations (Wu 2001, 2015, 2018, 2021; Finn et al. 1986; Finn and Wu 2013), and it was adopted for clayey soils (Boulanger 2019) although it is less available than for sandy soils.

By presenting the analysis methodology and results of the analyses using VERSAT-2D (WGI 2019), this case history study demonstrates the practicability of using the VERSAT approach and its capability of capturing the key features of seismic performance for earthen dams in earthquakes, even in large earthquakes. Dynamic analyses of the dam were performed using the proposed S_u/σ'_m approach for calculating in-situ undrained strengths as well as sensitivity analyses on input ground motion, phreatic surface, undrained strength, and dam bedrock foundation stiffness on dynamic response of the dam. The computed responses are found to be in good agreement with the measured dam crest settlements and the observed lateral spreading deformation pattern.

DAMAGES OF THE DAMS BY THE 1989 LOMA PRIETA EARTHQUAKE

Locations of Lenihan Dam and Austrian Dam are shown in Fig. 1(a). Lenihan Dam has a relatively flat 5.5:1 (horizontal to vertical) upstream slope; a plan view and cross section W-W' are shown in Figs. 1(b, c). In the 1989 earthquake, the dam developed longitudinal cracks on the dam faces; the dam crest had horizontal movements of about 62 mm (2.5 in) towards the downstream and settled 0.25 m (10 in) on average. The reservoir elevation at the time of the earthquake was very low, approximately 30 m below the spillway elevation; the phreatic surface shown in Fig. 1(c) was estimated using data from piezometers installed after the 1989 earthquake but observed when the reservoir level was low and equivalent to that during the earthquake (Dawson and Mejia 2021).

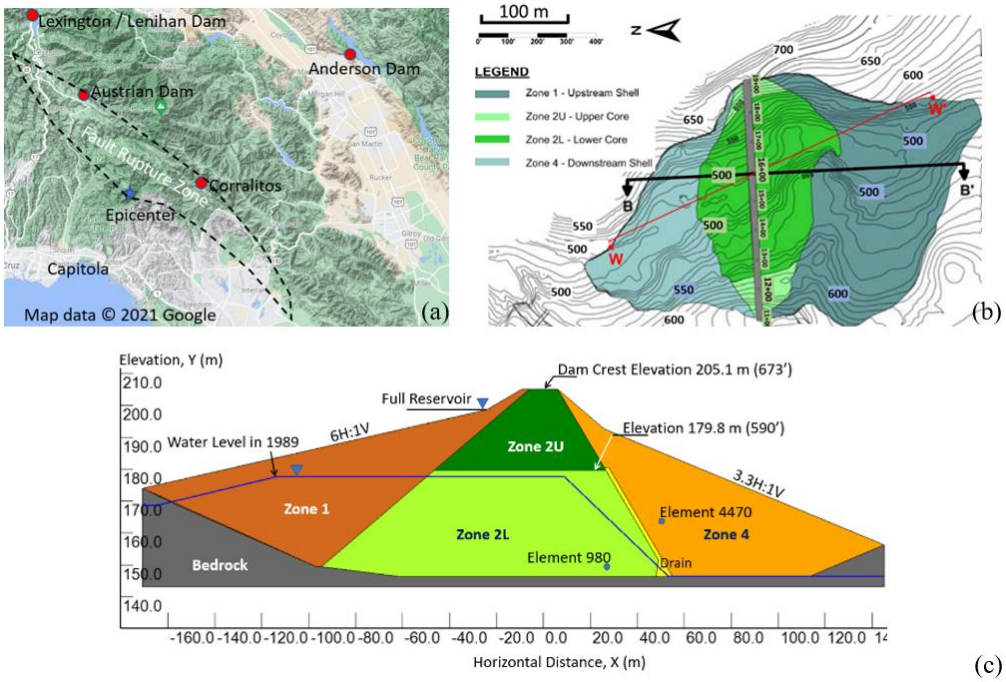

Figure 1. (a) Locations of the earthquake fault rupture zone, Lenihan and Austrian Dams; (b) Lenihan Dam plan view showing W-W' (Modified from SCVWD 2012.); (c). Lenihan Dam cross-section W-W' and a phreatic surface derived from Dawson and Mejia (2021).

The 230 m long Austrian dam was founded on bedrocks with crest width of 6.1 m and crest elevation of 343 m (Harder et al. 1998; Boulanger 2019). The dam's upstream and downstream slopes range from 2.5:1 near the crest, transitioned to 3:1 in the middle of the slopes, and further flatted to 3.5:1 near the toes. Post construction study and sampling of the dam fills indicated that there was no appreciable difference between the upstream and downstream zones, and the gravel drain was not completely effective in relieving the downstream seepage pressures. As such, it was considered reasonable to treat the entire dam consisting of homogeneous materials for analysis (Harder et al. 1998); the phreatic surface for the Austrian dam used in current analysis is estimated based on the water levels in piezometers measured on October 16, 1989 (before the earthquake). An analytical model of the dam's maximum cross section is shown latter in the paper in Fig. 7(a).

Located at 11 km from the earthquake epicenter, the Austrian dam was heavily damaged in the 1989 earthquake. Noticeably, the standpipe for piezometer P-1 (located midway down the downstream face) was observed to be significantly deformed between elevations 291.1 and 292.6 m (or about 7.6–9.1 m above the bedrock), and the standpipe for piezometer P-6 (located at the dam crest) was deformed between elevations 310.2 and 317.2 m (about mid-height of the dam). These movements were suggestive of earthquake-induced internal and deep deformations related to lateral spreading of the earthfill dam (Harder et al. 1998). In addition to an average dam crest settlement of 0.76 m, post-earthquake survey also indicated that the right abutment appeared to move downstream horizontally 458 mm relative to the left abutment.

EMBANKMENT DAM FILLS AND THE UNDRAINED SHEAR STRENGTH

Geotechnical properties of the dam fills are shown in Table 1 for Lenihan Dam. The data are from Harder et al. (1998) and SCVWD (2012); the latter is the owner of the dam. The data for Austrian Dam are primarily compiled from Wahler Associates (1979, 1990) and Harder et al. (1998).

Of particular interest to the current study are the data from the isotropically consolidated undrained (ICU) triaxial tests conducted on undisturbed tube samples extracted from the two dams. From the ICU triaxial test data, undrained shear strengths (S_u) were calculated; for example, the calculated S_u of Lenihan Dam Zone 2L are plotted in Fig. 2(a) against the consolidation stresses, σ'_{3c}. The S_u is defined as the shear stress on the eventual failure plane at failure (i.e., τ_{ff}), and failure occurs when the principal stress ratio (σ'_1 / σ'_3) reaches its peak in shearing. In common language, this is the shear stress of the point on a Mohr circle that touches the failure envelope; it is less than the maximum shear stress in the Mohr circle. For Lenihan Dam, ICU triaxial tests were carried for all four soil zones (Zones 1, 2U, 2L and 4), whereas only results for the high plasticity soils of Zone 2L are shown in here.

For the in-situ pre-earthquake stress conditions, except these with K_0 of 1.0, the soils are not isotropically consolidated. In the current study using the finite element method, the undrained shear strength of a saturated soil element is calculated using the following equation,

$$S_u = c + \sigma'_m \tan(\Psi) \tag{1}$$

$$\sigma'_m = (\sigma'_x + \sigma'_y + \sigma'_z) / 3 \tag{2}$$

where S_u is the undrained shear strength of a soil element; σ'_m is the mean consolidation pressure (or stress) at the soil element center prior to earthquake loading; σ'_x and σ'_y are the horizontal and

vertical consolidation stresses, respectively, in two-dimensional (2D) plane strain finite element analysis presented in this study; σ'_z is the horizontal consolidation stress in the direction perpendicular to the 2D plane. The cohesion (c) and the friction angle (Ψ) are undrained strength parameters that would either be obtained from in-situ shear tests or determined from undrained direct simple shear tests; for the current study, they are derived from the ICU triaxial test data.

Table 1. Geotechnical properties of dam fills of Lenihan Dam

	Zone 1	Zone 2U	Zone 2L	Zone 4
USCS classification	SC, CL	SC, GC	CH, SM-MH	SC, GC
Percent coarser than 4.75 mm (%)	27 (0-43)	33 (3-58)	6 (0-29)	32 (13-56)
Percent finer than 0.075 mm (%)	39 (19-97)	31 (16-53)	79 (29-97)	30 (15-63)
Liquid limit	33 (30-39)	37 (30-48)	62 (43- 70)	33 (22-46)
Plasticity index (PI)	15 (6-24)	17 (14-29)	35 (15- 48)	15 (6-29)
Water content (%)	15 (10.3-26.5)	11.9 (6.0-17.7)	24.1 (17.8-37.1)	11.9 (6.2-19.9)
Dry unit weight (kN/m^3)	18.8 15.0-20.8	18.8 17.0-20.7	15.7 14.1-17.5	19.5 15.8-22.5
Saturated unit weight (kN/m^3)	21.7	20.8	19.5	22.0
K (m/s) [a]	398	363	207	473
Effective stress, c′ (kPa)	0	0	0	0
Effective stress, φ' (°)	37.5	35.5	25.5	35
K_g [b]	3713	3065	1033	4717

Sources: Data from Harder et al. (1998) and Engineering Report No. LN-3 (SCVWD 2012).
[a] The shear wave velocity, V_s, is calculated using $V_s = K \bullet (\sigma'_y/P_a)^{0.25}$. [b] K_g is derived using equation (3) in this study.

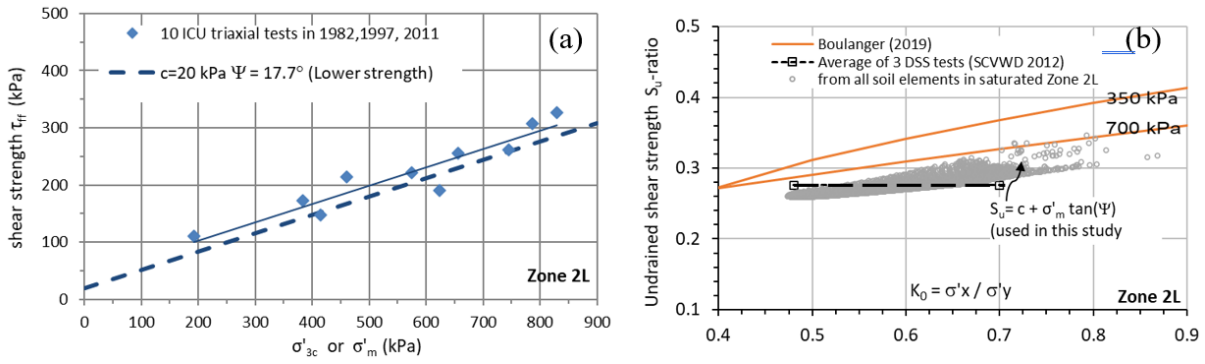

Figure 2. Lenihan Dam Zone 2L: (a) Undrained shear strength (S_u) derived from ICU triaxial test data; (b) Su-ratios ($=S_u/\sigma'_y$) used in here and compared with the DSS tests by SCVWD (2012)

Using the proposed S_u/σ'_m method, the computed S_u that are based on or referenced to the mean consolidation pressure (σ'_m) are compared in Fig. 2(b) with the S_u calculated using the procedure adopted by Boulanger (2019). The Duncan and Wright (2005) procedure for evaluating slope stability with limit equilibrium method was extended and applied by Boulanger (2019) for his finite difference dynamic analysis of the Austrian dam. In general, S_u calculated using the proposed S_u/σ'_m method are lower (and thus more conservative) than S_u calculated using the procedure adopted in Boulanger (2019). For the high plasticity Zone 2L soils of Lenihan Dam, the S_u-ratios applied in this study using the S_u/σ'_m method and the calculated σ'_m of soil elements are lower than these using Boulanger (2019) for the stress levels (σ'_y) of the dam's Zone 2L soils, i.e., 350-700 kPa as shown in Fig. 2(b); however, the S_u-ratios by the S_u/σ'_m method could be slightly higher than those by Boulanger should the stress levels are lower than 350 kPa (WGI 2022b) as S_u-ratios by Boulanger are function of both K_0 and stress level. The range of S_u-ratios agrees well with that obtained from direct simple shear (DSS) tests on three samples of Zone 2L soils (SCVWD 2012). The proposed S_u/σ'_m approach might be more suitable for engineering practice as shown in the following dynamic analysis.

STATIC STRESSES OF THE DAMS PRIOR TO THE EARTHQUAKE

The static stresses of the dams were calculated using the static analysis module of VERSAT-2D, whereas an elastic perfectly plastic model with the Mohr-Coulomb failure criterion is adopted. Prior to failure, the shear modulus is modelled as linear and strain-level independent; however, the stress-level dependency of soil stiffness (shear and bulk moduli) is allowed by using equations (3) and (4) for calculating the two moduli as are used for the dynamic analysis. Note that soil stiffness parameters used for computing the in-situ effective stresses of the dam prior to earthquake shaking are normally determined using the static and drained loading tests, such as oedometer tests or triaxial tests.

The finite element model for Lenihan Dam consists of 9122 soil elements (1.52 m wide and 0.91 m high each). The mesh for Austrian Dam contains 7072 soil elements. The construction sequence of the dam was modelled by building the dam in 5-m thick layers. The stress-level dependent elasticity moduli (soil stiffness) are updated after each 5-m thick layer is added onto the model. After completion of the dam construction to its crest, reservoir water levels and the phreatic surface were raised gradually in small increments. The incremental loading process (or unloading due to water buoyancy) is an essential analysis element needed to achieve the required convergence in a nonlinear analysis involving plasticity and flow rule. Each of the load increment was considered complete if the total unbalanced force of the entire model is less than 0.5 kN.

The phreatic surface (water table) was applied as a piezometric surface; the pore-water pressure was computed as the vertical distance from the piezometric line to the point of interest, multiplied by the unit weight of water. When there is no vertical seepage gradient, this approach is a reasonable approximation (USBR 2019). The calculated static stresses of Lenihan Dam are shown in Fig. 3(a) and Fig. 3(b) for vertical effective stresses (σ'_y) and coefficients of horizontal stresses ($K_0=\sigma'_x/\sigma'_y$), respectively, where σ'_x is horizontal effective stress.

The undrained shear strengths of the saturated soils were calculated using the proposed S_u/σ'_m approach in equation (1), whereas the σ'_m were calculated in equation (2) using the σ'_x, σ'_y, and σ'_z directly computed from the static analysis. The ratios of S_u/σ'_y are shown in Fig. 3(c).

DYNAMIC ANALYSIS OF EARTHEN DAMS: A TOTAL STRESS APPROACH

The nonlinear dynamic analysis is a continuation of VERSAT static stress analysis. The VERSAT dynamic analyses of seismic response are always carried out in an undrained condition, whereas a total stress analysis is performed for clayey soils using the VERSAT-CLAY model or an effective stress analysis is conducted for sandy soils using the VERSAT-SAND model; the latter can take into account the effect of PWP on shear strength of sandy soils (i.e., c' and φ') as the effective stresses decrease with the increase of PWP, and ultimately can model liquefaction of sandy soils. The VERSAT-SAND model had been adopted for modelling liquefaction of the hydraulic fills in the dynamic analysis of the Upper San Fernando dam (Wu 2001). When the VERSAT-CLAY model is used, the S_u are calculated using the pre-earthquake stresses (i.e., the static stresses), after which they are kept unchanged throughout the entire duration of earthquake loading. The VERSAT approach is in fact very similar to the limit equilibrium method for slope stability analyses; it requires no calibration of model parameters.

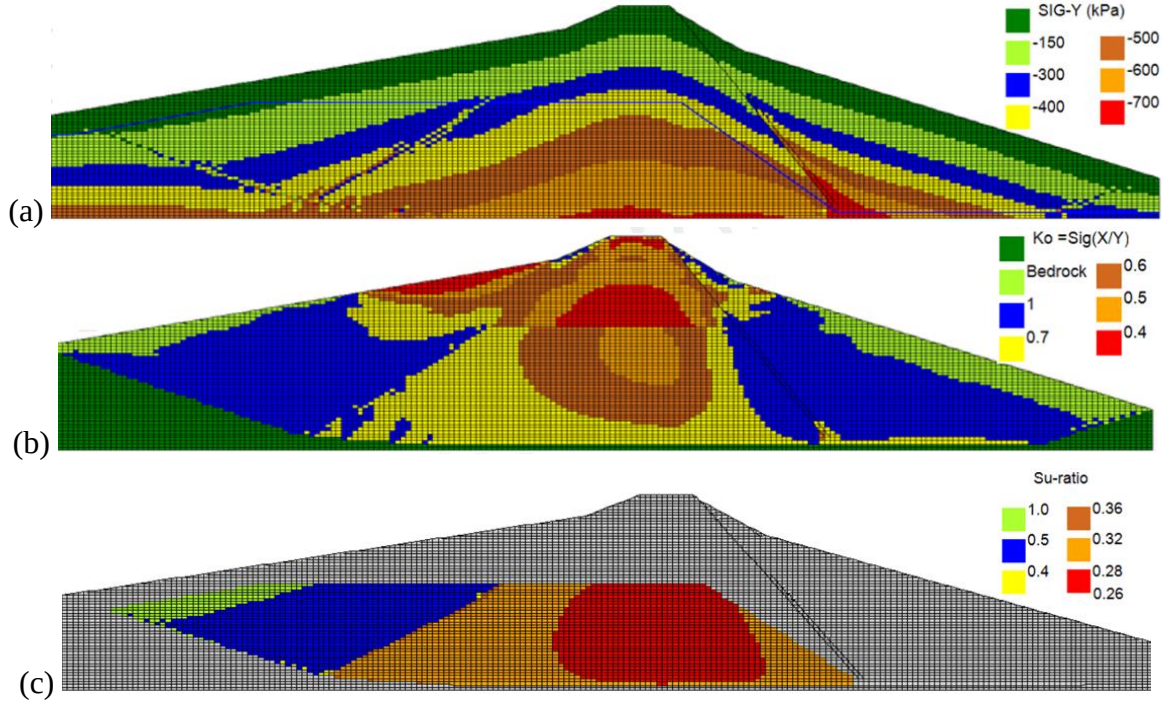

Figure 3. Lenihan Dam: (a) vertical effective stresses σ'_y; (b) horizontal stress coefficient K_0; (c) undrained shear strength ratio (Su-ratio = S_u/σ'_y).

Input Ground Motions

Strong ground motions from the 1989 earthquake were measured on the left abutment, left crest and right crest of the Lenihan dam. The recorded accelerations at the left abutment on bedrock are directly used in this case study of Lenihan dam; this earthquake record has horizontal PGAs of 0.44g and 0.41g, and a vertical PGA of 0.14g. In addition, the ground motions calculated from analyses of the Lenihan dam are compared with these recorded at the dam crest in the 1989 earthquake.

For the Austrian dam there was no reported data on shear wave velocities of the foundation bedrock, consisting of highly fractured sandstone, graywacke, cobble conglomerate, shale, and serpentine (Harder et al. 1998), but unpublished data from a limited number of other projects in the region have shown shear wave velocities ranging from 760 to 2,700 m/s in the upper 30 m of the Franciscan formation (Boulanger 2019). The motions at the Austrian Dam site were not recorded; they were estimated to have peak horizontal accelerations between 0.55 and 0.60g (Harder et al. 1998).

For analysis of seismic deformations of the Austrian dam in 1989, it is considered appropriate to linearly scaling up the ground motions recorded at left abutment of the Lenihan dam (i.e., the Lexington station in PEER database) and use the scaled motions as the input ground motions at the Austrian dam. The Lexington station was located further away from the epicenter than the Austrian Dam site (see Fig. 1a); it was outside of the surface projection area of the Loma Prieta fault rupture zone. In current ground motion calculation, the Lexington station was considered to be a foot-wall site, and it had R_{jb} of 3.22 km and R_{rup} of 5.02 km (PEER 2021). On Franciscan formation rocks with an inferred V_{s30} of 1,070 m/s, the recorded Lexington motions had an Arias intensity (AI) of 1.9 cm/s, peak horizontal accelerations of 0.41g in 90° and 0.44g in 0° (PEER 2021).

Using the input parameters discussed above and others (Mw = 6.93, Z_{TOR} = 3.8 km, Rx = -3.22 km for foot-wall site, V_{s30} = 1000 m/s which is the highest V_{s30} value allowed in the GMPEs), horizontal peak ground acceleration (PGA) at the Lexington station (the median value at 5% damping) was estimated to be 0.38g from the NGA West2 ground motion prediction equations (GMPE) and the associated weight of 0.12 for Idriss model and 0.22 for other four models (Bozorgnia et al. 2014). When the same calculation was carried out for the Austrian Dam site (a hanging-wall site), a PGA (also the median value at 5% damping) of 0.52g was estimated. The PGAs at the two sites predicted by the GMPEs of NGA West 2 are remarkably consistent with the measured 0.41-0.44g at the Lexington station or the estimated 0.55-0.60g at the Austrian dam; the predicted median PGAs at both sites are lower by about 11% than the recorded (or estimated) PGAs. The predicted PGA at the Austrian dam is approximately 36% higher than the predicted PGA at the Lexington station; therefore, the measured ground motions at the Lexington station were linearly scaled up by a factor of 1.36 and applied as the input motions at the Austrian dam. The scaled accelerations have horizontal PGAs of 0.56g and 0.60g for the 90° and 0°components, respectively, and vertical PGA of 0.19g. For finite element models having a rigid base, acceleration time histories (horizontal and vertical) are applied directly at the rigid base, i.e., assuming the input motions were recorded at the rigid base.

VERSAT-2D Soil Constitutive Models

Soil constitutive models for dynamic nonlinear analyses are comprised of the Mohr Coulomb failure criteria for simulation of soil shear strengths and the 2-parameter hysteretic shear stress-strain relationship for modelling of soil stiffness including shear modulus reduction and hysteretic damping increase with the increase of shear strains.

The hyperbolic stress - strain relationship is adopted for simulation of soil hysteresis loops. The low-strain shear modulus, G_{max}, and the bulk modulus, B, are stress level dependent as defined in the following:

$$G_{max} = K_g P_a \left(\frac{\sigma_m'}{P_a}\right)^m \quad (3)$$

$$B = K_b P_a (\frac{\sigma_m'}{P_a})^n \quad (4)$$

where P_a is the atmospheric pressure, 101.3 kPa; K_b is bulk modulus constant; K_g is shear modulus constant; m and n are shear and bulk modulus exponentials, respectively; σ_m' is defined in equation (2).

The relationship between the shear stress, $\tau_{xy,}$ and the shear strain, γ, for the initial loading condition is modelled to be nonlinear and hyperbolic as follows:

$$\tau_{xy} = \frac{G_{max}\,\gamma}{1+R_f \bullet |\gamma|} \quad (5)$$

$$R_f = \frac{G_{max}}{\tau_{ult}} \quad (6)$$

where τ_{ult} is the ultimate shear stress in the hyperbolic model; G_{max} is the low-strain shear modulus ($G_{max} = \rho V_s^2$ with ρ being the soil density and V_s being the shear wave velocity).

The τ_{ult} is conveniently determined by introducing a modulus reduction factor R_f, which is shown in equation (6) and detailed in Wu (2001). As noted in Finn and Wu (2013), the use of R_f enhances the hyperbolic stress-strain model so that the model can provide a better match to the target dynamic modulus (G) and damping data. For an example, at a shear strain of 0.1%, the G/G_{max} ratio is 0.5 and the hysteretic damping is 14.5% when R_f value is 1000; they become 0.33 and 22.4%, respectively, when R_f increases to 2000.

The shear stress-strain hysteresis response (simulated using the VERSAT-CLAY model) of soil elements subject to constant stress cyclic (sine wave) undrained loading are presented in Fig. 4. It is seen that numerical modelling can effectively simulate the cyclic response of soils as observed in a laboratory test or experienced in the field during an actual earthquake. In Fig. 4(a), when there is no static shear stress (e.g., a generic soil element within a level ground), sine-type input shear stresses do not cumulate strains (or displacements) on the soil element if the applied shear stress amplitude is less than the shear strength. When failure of the soil element occurs by applying cyclic stresses with an amplitude of 185 kPa, permanent shear strains cumulate.

The response of soil elements situated on soil slopes with initial static shear stresses is illustrated in Figs. 4(b, c, d) using soil elements 980 and 4470 on the Lenihan dam; see Fig. 1(c) for their locations on the dam. In this simulation, the dam is subject to two levels of sine-wave accelerations (frequency of 1.0 Hz) at its base, a moderate level with a PGA of 0.2g and a high level with a PGA of 0.3g. In Fig. 4(b), soil element 980 fails in the direction of the static shear stress, causing the element to deform to a new permanent configuration. The portion of stress exceeding the S_u is redistributed to adjacent soil elements, and progressively carried on to other elements if the immediate soil element also fails in shear. The amount of irrecoverable shear strain Δ-strain in Fig. 4(b) that is caused by a loading cycle depends on both magnitude and duration of the loading cycle. The pattern of irrecoverable displacement on soil elements with non-zero static shear stress is somewhat similar to that of a sliding block on inclined plane.

Figs. 4(c, d) show 4-cycle response of soil elements 980 and 4470 subject to the high level of sine-wave accelerations with PGA of 0.3g, indicating much larger shear strains than for PGA of 0.2g. Under 0.3g, in Fig. 4(c) the level of cyclic shear stresses could be high enough to cause a near-failure stress condition in the opposite direction to the initial static shear stress. Each hysteresis loop for element 980 has a double strain amplitude of up to 0.25%, indicating a

reasonable amount of hysteretic damping. The shear stress and strain loops in Fig. 4(d) for soil element 4470, located in the unsaturated Zone 4 soils, are typical response of frictional soils modelled using the VERSAT-SAND model.

SEISMIC DEFORMATIONS OF LENIHAN DAM

The soil parameters for dynamic analyses of Lenihan Dam included viscous damping of 2%, $R_f = 0.75*K_g$ (see Table 1 for K_g); for saturated Zone 2L, c = 20 kPa and Ψ = 17.7° were derived for calculation of S_u in equation (1), and c = 20 kPa and Ψ = 23.7° were used for saturated Zone 1.

The horizontal displacement contours in Fig. 5(a) indicate that the dam deforms in two opposite directions from the central part of the dam. The lateral spreading movements of the dam body caused the dam to settle. The dynamic analysis calculated dam crest displacements of 0.06 m and -0.26 m (horizontal and vertical) using the LEX-00° horizontal and its associated vertical input accelerations; the calculated crest displacements are 0.13 m and -0.27 m (horizontal and vertical) using the LEX-90° horizontal and its associated vertical input accelerations. The computed dam crest settlements of 0.26-0.27 m are in good agreement with the actual dam crest settlement of 0.25 m observed immediately after the 1989 earthquake.

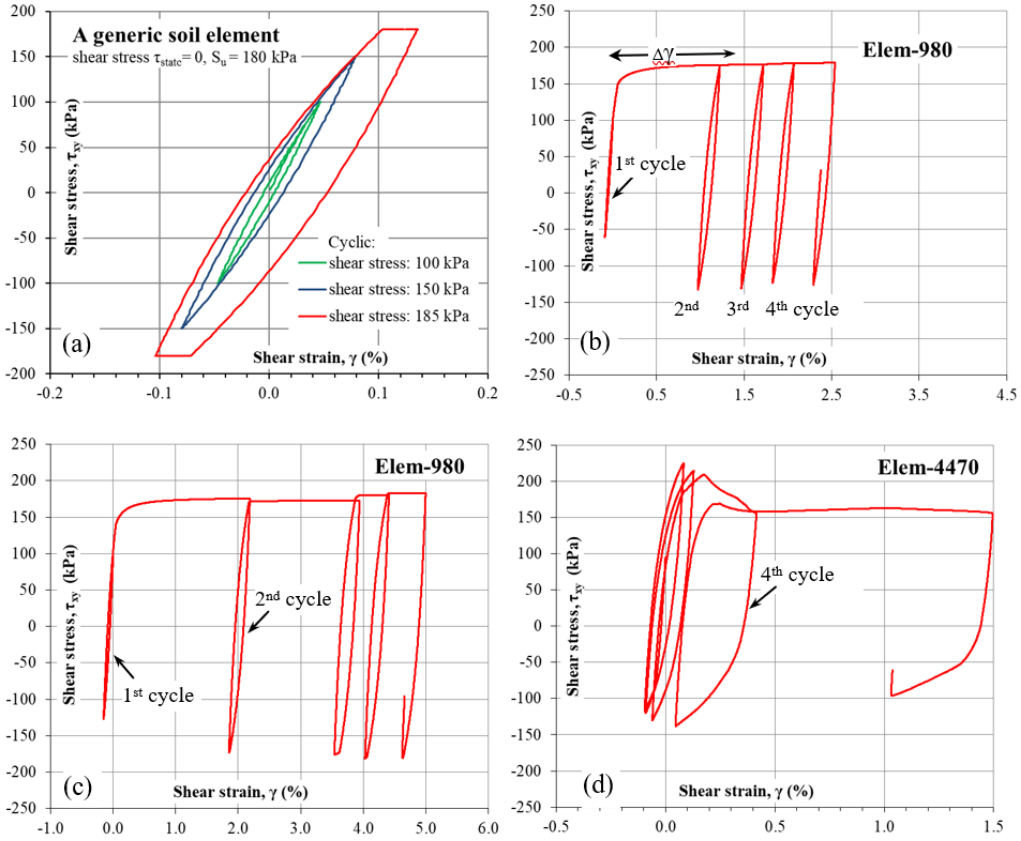

Figure 4. Shear stress-strain response in constant shear stress amplitude cyclic (sine wave) loading: (a) for a generic soil element (τ_{st} = 0, S_u=180 kPa); (b) for soil element 980 (τ_{st} = 102 kPa) under the 0.2g input accelerations; (c) for soil element 980 under the 0.3g input accelerations; and (d) for soil element 4470 in unsaturated Zone 4 under the 0.3g input accelerations.

The deformation pattern of the dam is consistent with the computed shear strains of the dam, as shown in Fig. 5(b). Similar to observations of clay embankment in a limit equilibrium stability analysis, significant shear straining zone tends to develop first near the bottom of a slope due to high shear stresses. Shear strains between 1.5 and 3% were predicted to have occurred in the lower part of the upstream slope, i.e., in the saturated dam fills immediately above the bedrock. Soil elements in a large area near the bottom of the high plasticity soils (Zone 2L) under the downstream slope were predicted to have shear strains between 3 and 5%.

The computed time histories of horizontal (DIS-X) and vertical (DIS-Y) displacements at the dam crest are shown in Fig. 6(a). The graph also includes for comparison the computed horizontal displacements at the mid-height (node 7943) of the downstream slope of the dam. The analyses predicted, at the end of earthquake the dam crest moves 60 mm and node 7943 moves 200 mm, both horizontally and in the downstream direction. Majority (about 0.25 m) of the crest settlement (DIS-Y) was predicted to have occurred, as expected in an undrained total stress analysis, during the early 10 s of shaking; in reality, settling of the dam may have continued during shaking after 10 s.

The 5% damped response spectra of the computed horizontal accelerations (PGA of 0.47g) at the dam crest of Lenihan Dam are shown in Fig. 6(b); the results indicate a peak spectral acceleration (S_a) of 1.78g at 1.0 s and a second peak S_a = 1.5g at 0.5 s. The spectral peaks agree well with the recorded (or measured) accelerations (PGA of 0.45g) at the dam crest that have a peak S_a = 2.25g at 1.0 s and a second peak S_a = 1.1g at 0.5 s.

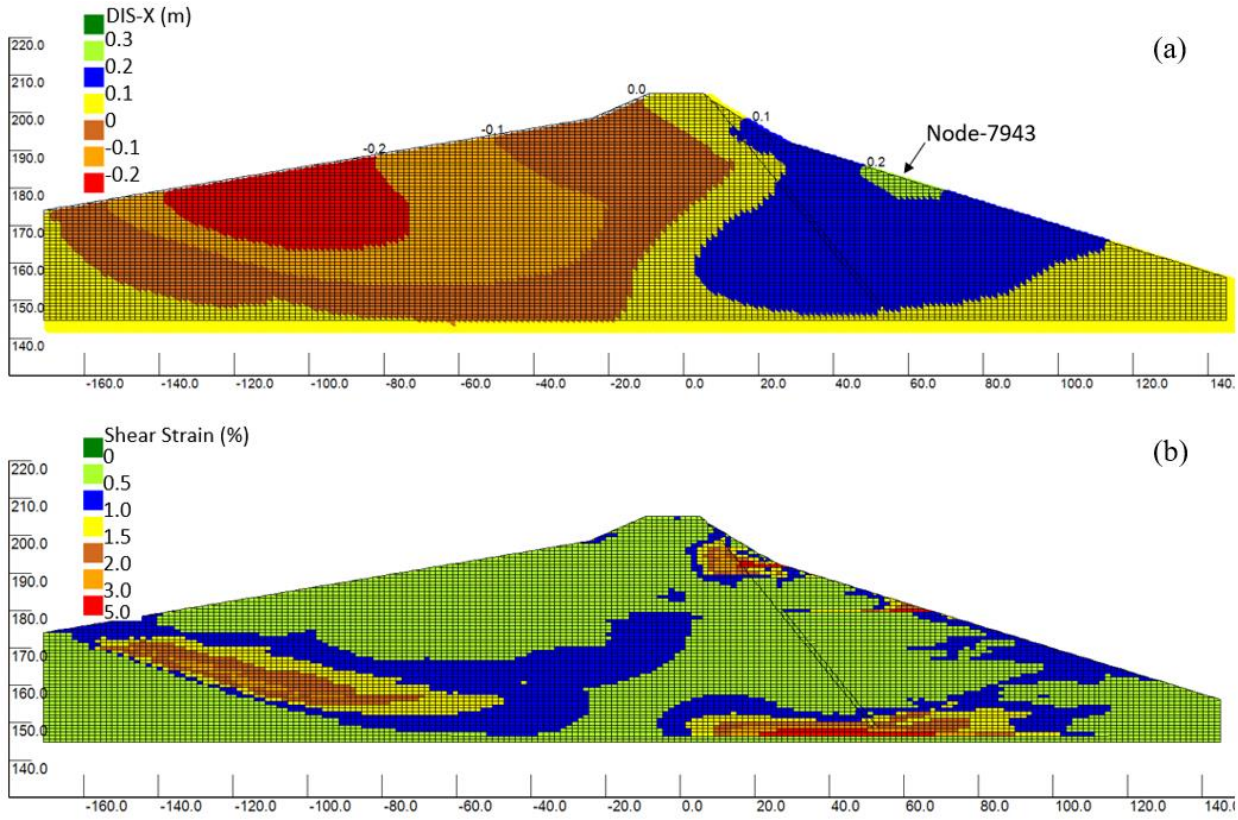

Figure 5. Lenihan Dam at end-of-earthquake (a) contours of horizontal (DIS-X) displacements; and (b) contours of absolute shear strains, |γ| (%).

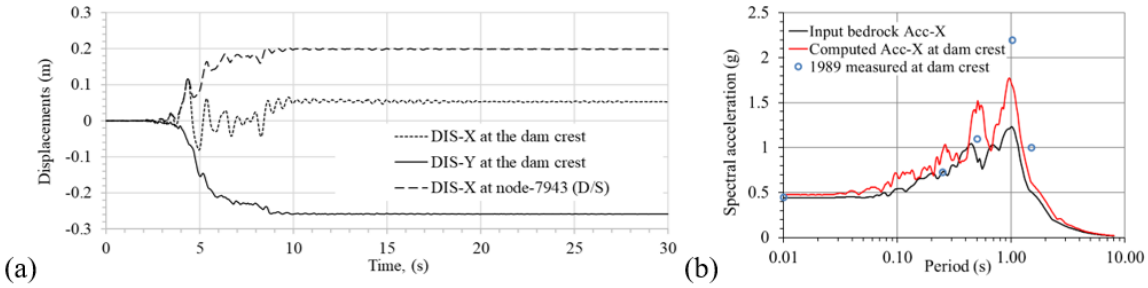

Figure 6. Lenihan Dam: (a) displacement time histories; (b) Response spectra (5% damped)

SEISMIC DEFORMATIONS OF AUSTRIAN DAM

The soil parameters for dynamic analyses of the Austrian dam included viscous damping of 1%, Rf = 500, DT = 0.001 s, c = 14 kPa and Ψ = 22° in equation (1) for saturated dam fill, φ' = 44° for unsaturated dam fill, and K_g = 2647 for both saturated and unsaturated fills (Harder et al. 1998). The recorded accelerations (LEX-00°, LEX-90°, and their associated vertical component) were linearly scaled up by a factor of 1.36 and then applied as rigid-base input motions.

The basic pattern of deformations is that the upstream part of the dam moves laterally toward the reservoir and the downstream part of the dam moves laterally but in the opposite direction. Similar pattern to Lenihan Dam, the lateral spreading movements of the dam body caused the Austrian dam to settle. The dynamic analysis calculated a dam crest settlement of 0.77 m using the LEX-00° horizontal and its associated vertical input accelerations; the calculated crest settlement was 0.70 m using the LEX-90° horizontal and its associated vertical input accelerations. The computed dam crest settlements are in good agreement with the actual dam crest settlement of 0.76 m observed immediately after the 1989 Loma Prieta earthquake. The computed horizontal displacements are about 0.72-0.58 m (for LEX 00°-90°) on the upstream slope moving towards the reservoir; they are about 0.49-0.54 m (for LEX 00°-90°) on the downstream slope.

Again, the deformation pattern of the dam is consistent with the computed shear strains of the dam, as shown in Fig. 7(a). Shear strains between 5 and 10% were predicted to have occurred in the lower part of the upstream slope, i.e., in the saturated dam fills immediately above the bedrock; in it one soil element was predicted to have shear strain greater than 10%. The shear strains of the saturated dam fills in the downstream slope of the dam are of a similar order of magnitude, also about 5-10%; however, in a small zone near the base of the downstream slope, the shear strains are large at about 15-20% and greater than 20% at the zone's bottom. This downstream shear zone (i.e., the zone with shear strains larger than 10%) is in relatively lower ground (low elevation); the ground elevation in this shear zone is about 10 m lower than the shear straining zone in the upstream slope of the dam.

The computed horizontal displacements and shear strains are consistent and in great agreement with the observed dam performance in the 1989 earthquake, in terms of the magnitude and location of "lateral spreading of the embankment of the dam" (Harder et al 1998) and the apparent deformations observed in standpipe of piezometers on downstream of Austrian Dam.

Parametric analyses of the Austrian dam were conducted and presented in WGI (2022a). A parametric study presented following is the method of applying the undrained shear strength of

the saturated dam fills in dynamic analysis. The S_u/σ'_m approach has been used as the default method for the foregoing analyses. In this sensitivity analysis, the total stress envelope parameters (c, φ) will be used to represent the undrained shear strengths of the saturated dam fills. In here, the strength parameters (c, φ) are derived from the total stress Mohr-Coulomb failure envelope; these parameters are sometimes reported in literature (Harder et al. 1998; Bray and Macedo 2019) to represent undrained shear strength of soils, and they are often used in static analysis of highly over-consolidated soils and less frequently for seismic stability evaluation of earthen dam.

In here, dynamic analyses were carried out using the "Total Stress" analysis option and the VERSAT-SAND constitutive model for the total stress envelope approach (i.e., the c-φ approach) of the saturated dam fill. The analyses were conducted using the Case 2 phreatic surface and the Lower strengths with c = 14 kPa and φ = 21°. Note that these total stress envelope parameters (c, φ) were also reported in Harder et al. (1998) and referenced in Bray and Macedo (2019) in their illustrative example for estimating earthquake induced slope displacements.

Results of the two analyses are presented in Table 2. When the Corralitos[1] rigid-base input accelerations were applied in the c-φ approach, the calculated dam crest settlements increase to 2.40-1.30 m (for CLS 00°-90° and the c-φ approach in 2b) that are about 3-2 times the settlements of 0.77-0.68 m (for CLS 00°-90° and the S_u/σ'_m approach in 2a). The shear strain contours of the dam computed using the c-φ approach are shown in Fig. 7(b) (for CLS-00° input accelerations) for comparison of shear strain distribution in the dam in Fig. 7(a) (for LEX-00° input accelerations and the S_u/σ'_m approach). The color legend for shear strains in the two figures is purposely made different to be able to show the difference in magnitude of strains between the two analysis cases. For a large area in the upstream embankment slope of the dam, the shear strains increase to 20-30% when the c-φ approach was adopted, see Fig. 7(b); in the same area the shear strains are about 5-10% (in the yellow color zone in Fig. 7(a)) for the S_u/σ'_m approach.

The too large dam crest settlement and too large lateral displacements (up to 1.8 m) on the dam face slopes calculated using the Corralitos input accelerations, as seen in Fig. 7(c), are mainly attributed to the high vertical accelerations with a PGA of 0.46g (i.e., 71% and 95% of the PGAs for the 0° and 90° horizontal accelerations, respectively) in the recorded Corralitos record. The high vertical input accelerations could significantly reduce the vertical total stresses (σ_y), thus reduce the principal total stresses (σ_1 and σ_3) and ultimately reduce the shear resistance of the saturated dam fills, on both the upstream and downstream slopes of the dam.

This sensitivity dynamic analysis suggested that the c-φ approach may be used in dynamic analyses of earthquake deformations of saturated cohesive soils, provided that the input motions don't contain large vertical accelerations such as the Lexington record. The Lexington record had vertical accelerations with a PGA of 0.19g that was about 32-35% of the PGAs for the two horizontal accelerations. However, cautions must be taken in interpreting the data and analysis results when the c-φ approach is indeed adopted, even if it is a sensitivity analysis.

[1]Both the Austrian dam site and the Corralitos station were situated near the top edge of the Loma Prieta fault rupture zone (a reverse oblique fault). The unscaled accelerations recorded at Corralitos (PEER 2021) are used here.

Table 2. Computed Accelerations and displacements at ground surface of Austrian Dam

Cases	Details	Input motions	Dam crest			Downstream DIS-X at P-6, m
			ACC-X, g	DIS-X, m	DIS-Y, m	
CASE 1: phreatic surface as in piezometers P-6, P-4, P-1	1a. Lower S_u applied using the S_u/σ'_m approach (c = 14 kPa, Ψ=22°)	LEX-00	0.66	-0.19	-0.77	0.49
		LEX-90	-0.63	-0.03	-0.70	0.54
		CLS-00	1.13	-0.01	-0.69	0.51
		CLS-90	1.21	-0.06	-0.63	0.45
CASE 2: Phreatic surface 4 m higher than measured at P-4	2a. Lower S_u applied using the S_u/σ'_m approach (c = 14 kPa, Ψ=22°)	CLS-00	1.12	0.01	-0.77	0.58
		CLS-90	1.15	-0.04	-0.68	0.50
		LEX-00	0.61	-0.18	-0.83	0.54
		LEX-90	0.57	-0.02	-0.75	0.58
	2b. Lower S_u using the total stress c-φ approach (c = 14 kPa, φ=21°)	CLS-00	0.75	-0.59	-2.40	1.16
		CLS-90	0.98	-0.60	-1.30	0.53
		LEX-00	0.64	-0.42	-0.84	0.41
		LEX-90	0.67	-0.14	-0.78	0.52

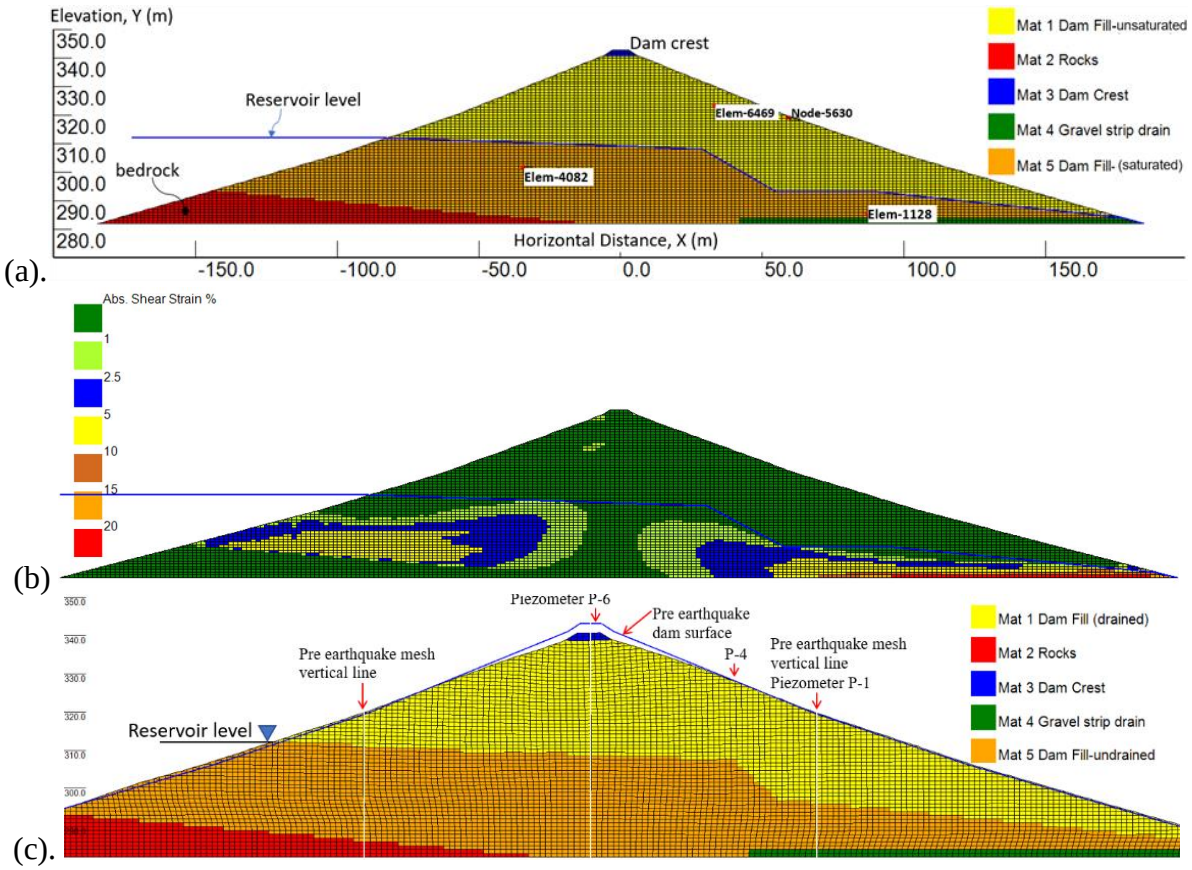

Figure 7. Austrian Dam: (a) VERSAT-2D model with soil and rock zones, reservoir water level and phreatic surface; (b) end-of-earthquake contours of |γ| (%) for Case 1a; and (c) end-of-earthquake deformed dam for Case 2b showing dam crest settlement of 2.4 m.

CONCLUSIONS AND DISCUSSION

Two-dimensional (2D) plane strain total stress dynamic analyses of the Lenihan and Austrian dams under the 1989 Loma Prieta earthquake were conducted using the VERSAT-CLAY model for simulation of the undrained response of saturated dam fills within the total stress approach; the VERSAT-SAND model was adopted for modelling the unsaturated dam fills above the phreatic surface. In this case history study of the two dams, the dynamic analyses were able to predict dam crest settlements that are in good agreement with these observed during the earthquake. Noticeably, a piezometer tube (installed on the midway of the downstream slope of the Austrian dam) deformed significantly at a location about 8 m above the bedrock foundation; the shear displacement suggested that the dam had deep deformations related to lateral spreading of soils due to shear failure. Results of this study revealed this mechanism of dam deformations, i.e., large shear strains occurred near the bottom of the dam slopes.

The dynamic analyses showed that the proposed S_u/σ'_m approach for calculating the undrained strengths of the saturated dam fills provides reasonable conservatism for engineering analysis and design. The calculated dam crest settlements in the range of 0.70-0.83 m for Austrian Dam are in good agreement with the measured average of 0.76 m; for Lenihan Dam, the computed dam crest settlements range from 0.22-0.35 m that also agree with the measured average of 0.25 m. Parametric analyses demonstrated the significance of S_u on dam performance and revealed limitations in using the total stress envelope c-φ approach for characterizing the undrained strengths of cohesive soils; it is suggested that the c-φ approach be avoided whenever possible for dynamic analysis of dams and be excluded if the analysis involves large vertical input accelerations.

There are two noticeable uncertainties facing the case study of the Austrian dam: the uncertainty on input ground motions and the uncertainty on undrained shear strength characteristics of the saturated dam fill. The actual ground motion experienced by Austrian Dam in 1989 can significantly differ from what were used in this study, and there is lack of in-situ test data for characterization of the aleatory variability of undrained shear strengths of the saturated dam fills.

Uncertainties related to the case study of Lenihan Dam (see WGI 2022b) would include effect of the topography of the dam's rock foundation on ground motions propagating from the bedrock to the dam body. Previous studies by others (Hadidi et al. 2014; Dawson and Mejia 2021) appear to have significantly underpredicted the crest settlement of the dam under the 1989 earthquake. For the case of the 2D plane strain dynamic analyses by Hadidi et al. (2014), the underestimate of crest settlement could be the alignment of cross section B-B' in Fig. 1(b) adopted in their study; the bedrock surface there is noticeably higher in elevation and more irregular than currently used in this study. For the case of the 3D dynamic analysis by Dawson and Mejia (2021), they suggested that it is possible that post seismic consolidation of the lower core (Zone 2L) contributed to the measured crest settlement.

ACKNOWLEDGMENTS

The anonymous reviewers provided valuable comments and suggestions related to input ground motions and discussions on the undrained response of saturated clayey soils that significantly improved the paper. Engineers of the Santa Clara Valley Water District in California provided access to engineering data for Lenihan Dam. The author sincerely thanks them for their supports.

REFERENCES

Boulanger, R. W. 2019. "Nonlinear dynamic analyses of Austrian Dam in the 1989 Loma Prieta earthquake." *J. Geotech. Geoenviron. Eng.* 145 (11).

Bozorgnia, Y., et al. 2014. "NGA-West2 research project." *Earthquake Spectra* 30 (3): 973–987.

Bray, J. D., and J. Macedo. 2019. "Procedure for estimating shear-induced seismic slope displacement for shallow crustal earthquakes." *J. Geotech. Geoenviron. Eng.* 145 (12).

Dawson, E., and L. Mejia. 2021. Three-dimensional analysis of the Lenihan dam for the Loma Prieta earthquake. In *Proc. 2021 Annual United States Society of Dams Conference*.

Duncan, J. M., and S. G. Wright. 2005. *Soil strength and slope stability*. New York: Wiley.

Finn, W. D. L., and G. Wu. 2013. "Dynamic analyses of an earthfill dam on over-consolidated silt with cyclic strain softening." In *Proc., 7th Int. Conf. on Case Histories in Geotechnical Engineering*, Keynote paper, edited by S. Prakash. Chicago.

Harder, L. F., Jr., J. D. Bray, R. L. Volpe, and K. V. Rodda. 1998. "Performance of earth dams during the Loma Prieta earthquake." In *US Geological Survey Professional Paper 1552-D*, edited by T. L. Holzer, 3–26. Washington, USGS.

Hadidi, R., Y. Moriwaki, J. Barneich, R. Kirby, and M. Mooers. 2014. "Seismic deformation evaluation of Lenihan Dam under 1989 Loma Prieta Earthquake." In *Proc. 10th US National Conf. on Earthquake Engineering, Frontiers of Earthquake Engineering*. Oakland, CA: Earthquake Engineering Research Institute.

Ladd, C. C., and R. Foote. 1974. "New design procedure for stability of soft clays." *J. Geotech. Eng.* 100 (7): 763-786.

PEER (Pacific Earthquake Engineering Research Center). 2021 PEER Ground Motion Database. https://ngawest2.berkeley.edu. California.

Sweeney, N., and L. Yan. 2014. "Dam safety upgrade of the Ruskin dam right abutment." In *Proc. 2014 Annual CDA Conference*. Alberta.

SCVWD (Santa Clara Valley Water District). 2012. Seismic stability evaluations of Lenihan Dam: Site characterization, material properties, and ground motions. Report No. LN-3, Santa Clara Valley Water District, California.

USBR (US Bureau of Reclamation). 2019. *Best Practices in Dam and Levee Safety Risk Analysis - Chapter D-5 Embankment Slope Instability*. USBR.

Wahler Associates. 1979. Initial evaluation of seismic stability of Austrian Dam, December 1979. File No. 622-13, Item No. 8. Sacramento, California Dept. of Water Resources.

Wahler Associates. 1990. *Austrian dam-investigation and remedial construction following the October 17, 1989 Loma Prieta Earthquake: Report prepared for the San Jose Water Company*. California.

Wu, G. 2001. "Earthquake induced deformation analyses of the Upper San Fernando dam under the 1971 San Fernando earthquake." *Can. Geotech. J.* 38 (1): 1-15.

Wu, G. 2015. "Seismic design of dams." In *Encyclopedia of Earthquake Engineering*, Berlin Heidelberg, Germany: Springer-Verlag.

Wu, G. 2018. "Probabilistic approach to design of seismic upgrade to withstand both crustal and subduction earthquake sources." In *Proc., 25th Vancouver Geotechnical Society (VGS) Annual Symposium on Ground Improvement*. BC, Canada.

Wu, G. 2021. "Reliability-based dynamic analyses for seismic design optimization in British Columbia." In *Proc., 27th VGS Annual Symposium on Risk and Liability*. BC, Canada.

WGI (Wutec Geotechnical International). 2019. *VERSAT-2D v.2019: A computer program for 2-dimensional static and dynamic finite element analysis of continua*. BC, Canada.
WGI (Wutec Geotechnical International). 2022a. Finite Element Dynamic Analyses of Austrian Dam. Engineering Report No. WGI-220224 http://www.wutecgeo.com/publication.aspx.
WGI (Wutec Geotechnical International). 2022b. Case Study of Lenihan Dam under the 1989 Loma Prieta Earthquake. Engineering Report No. WGI-220301.